Proceeding of the 2004 American Control Conference
Boston, Massachusetts June 30 - July 2, 2004

Nonlinear Observer Design for Fuel Processing Reactors in Fuel Cell Power Systems

Haluk Görgün Murat Arcak
Rensselaer Polytechnic Institute, Troy, NY

Subbarao Varigonda Scott A. Bortoff
United Technologies Research Center, East Hartford, CT

Abstract— **This paper presents nonlinear observer designs for the Catalytic Partial Oxidation (CPO) and the Water Gas Shift (WGS) reactors in fuel cell power systems. The observers make use of available temperature and total pressure measurements and estimate the mole fractions of each species in the reactors. Estimation of H_2 and CO fractions is particularly useful for monitoring and control of the fuel processor. An advantage of our designs is that they are based on the reaction invariants and do not rely on knowledge of reaction rate expressions.**

I. Introduction

Fuel cell technology is highly promising for power generation with low emissions and high efficiency in stationary and automotive applications. A typical fuel cell system consists of a fuel processing system (FPS), a cell stack assembly, and a power conditioning unit, as presented in the books [3], [8], [11]. The cell stack is fed by the FPS, which reforms natural gas, gasoline, or other hydrocarbons, into hydrogen. In the cell stack, oxygen from the cathode channel reacts with the hydrogen from the anode channel to generate electricity. Among the most challenging control problems in fuel cell power systems is the regulation of hydrogen supplied from FPS to the cell stack in the presence of fast-varying electrical load. Insufficient supply of hydrogen from the FPS causes "starvation" of the cell, which means that the platinum catalyst will start consuming the graphite used in anode flow fields. Excessive hydrogen output from FPS reduces efficiency of the system, and is also undesirable. Likewise, carbon monoxide concentration must be maintained below a critical limit, because it poisons the catalyst surface by adsorbing on the active sites and blocking access to hydrogen.

Effective monitoring and control of H_2 and CO levels requires either measurements or reliable estimates of these variables. Due to the limitations of available sensors for these species [7], our approach in this paper is to estimate them with model-based observers. In our earlier study [1], we have developed a hydrogen observer design for the anode channel of the cell stack based on voltage measurements. However in this design FPS dynamics were not modelled, and their effect on the anode dynamics were treated as plant uncertainty. In this paper we study the FPS dynamics, and estimate not only hydrogen but also other species in its reactors, including CO.

There have been numerous studies to design observers for chemical reactors, as surveyed by Soroush [17]. Among them are Limqueco *et al.* [13], [12] and Iyer and Farell [9], who apply the differential geometric design procedure of Krener and Isidori [10] when only temperature is available for measurement. Their applications, however, are restricted to first-order reactors. Other designs, such as Gauthier *et al.* [5] and Gibon-Fargeot *et al.* [6], restrict the reaction rates by linear growth assumptions, and proceed with high-gain observer constructions. Soroush [16] allows nonlinear reaction rates, but assumes only one of the reactants is unmeasured. A further shortcoming of these observers is that they assume knowledge of reaction rates, which may not be available precisely.

In this paper we present a new nonlinear observer design that does not rely on knowledge of kinetic equations, but only on stoichiometric coefficients and available temperature and pressure measurements. The main idea is to use a change of coordinates that cancel the reaction rate expressions, and to proceed with a reduced-order observer construction with the new coordinates. A similar design has been presented

The work of the first two authors was supported in part by the National Science Foundation under grants ECS-0226094 and ECS-0238268.

Author for correspondence. Electrical, Computer and Systems Engineering Dept., Rensselaer Polytechnic Institute, 110 8^{th} St. Troy, NY. Email: arcakm@rpi.edu; Fax: (518) 276-6261; Tel: (518) 276-6535.

0-7803-8335-4/04/$17.00 ©2004 AACC

in Bastin and Dochain [2, Section 3.3], where the authors rely on flow measurements, and obtain linear observer error dynamics. In our design, however, the error dynamics are nonlinear because we do not assume availability of flow measurements and, instead, employ nonlinear orifice equations to calculate flows from pressure measurements. We further take into account temperature dynamics, which are not considered in [2].

This paper is organized as follows: In Section 2, we review the fuel processing system and present dynamic models of the CPO and WGS reactors. In Section 3, we present our observer designs for both reactors. Simulation results are given in Section 4, followed by conclusions in Section 5.

II. Fuel Processing System (FPS)

The FPS reforms hydrocarbons into a hydrogen-rich gas, and cleans harmful byproducts according to fuel cell requirements [4], [11], [15]. Among several reformer types, such as *steam reforming*, *autothermal reforming*, etc., in this paper we address the *catalytic partial oxidation* (CPO), which extracts hydrogen from the hydrocarbon fuel. A byproduct of this reactor is carbon monoxide, which is harmful for the cell stack, and is eliminated with a series of water gas shift (WGS) and preferential oxidation (PROX) reactors. (The latter is also known as *selective oxidation*). In this paper we only study the CPO and WGS reactors, because they contribute to the generation of hydrogen, which is the main variable we are interested in. However, the same design technique can be applied to the PROX to estimate other variables, such as carbon monoxide.

A. Catalytic Partial Oxidation (CPO)

The two main reactions in the CPO are Partial Oxidation (POX):

$$CH_4 + \frac{1}{2}O_2 \rightarrow CO + 2H_2\,, \tag{1}$$

and Full Oxidation (FOX):

$$CH_4 + 2O_2 \rightarrow CO_2 + 2H_2O\,. \tag{2}$$

Partial oxidation produces hydrogen for the cell stack, but also generates carbon monoxide which causes the poisoning phenomena in the cell stack. Full oxidation is useful because it supplies additional heat, which facilitates the partial oxidation reaction.

The reaction rate expressions for full- and partial-oxidation are given by

$$r_{pox} = s\, r_T \tag{3}$$
$$r_{fox} = (1-s)\, r_T, \tag{4}$$

where s is a selectivity variable which depends on the air-fuel ratio [14], and r_T is the total reaction rate given by the empirical expression

$$r_T = k_g[O_2]\frac{[CH_4]}{[CH_4]+\varepsilon}, \tag{5}$$

in which $[O_2]$ and $[CH_4]$ represent molar concentrations of oxygen and methane, respectively, and k_g and ε are coefficients available from empirical studies. The first term, $k_g[O_2]$, in (5) represents the oxygen mass transfer rate from gas phase to the catalyst. The second term, $\frac{[CH_4]}{[CH_4]+\varepsilon}$, accounts for the transient case where methane is the limiting reactant. We emphasize, however, that this reaction rate expression is not used in observer design, but only in simulations. The observer design is unchanged even if a different reaction rate is employed.

Denoting by M the vector of molar holdups of each species; that is,

$$M = ([N_2], [CH_4], [CO], [CO_2], [H_2], [H_2O], [O_2])'$$

we obtain from mole balance equations the dynamic model

$$\dot{M} = F_{fuel} + F_{air} - F_{out} + q_1\, r_{pox}\, V + q_2\, r_{fox}\, V \tag{6}$$

where, F_{fuel}, F_{air}, F_{out} (mole/sec) are the fuel, air and exit molar flow vectors respectively, $V(m^3)$ is the reactor volume, and q_1 and q_2 are obtained from the stoichiometry of the reactions (1) and (2):

$$q_1 = [0 \quad -1 \quad 1 \quad 0 \quad 2 \quad 0 \quad -\frac{1}{2}]' \tag{7}$$
$$q_2 = [0 \quad -1 \quad 0 \quad 1 \quad 0 \quad 2 \quad -2]'. \tag{8}$$

Likewise, from an energy balance principle, the dynamics of temperature T is given by

$$(mc_p)\dot{T} = {F_{fuel}}' h(T_{fuel}) + {F_{air}}' h(T_{air}) \tag{9}$$
$$-{F_{out}}' h(T) + \Delta H_{pox}\, r_{pox}\, V + \Delta H_{fox}\, r_{fox}\, V,$$

where T is the reaction temperature (K), m(kg) and c_p(kJ/kg K) are mass and specific heat capacity of the catalyst bed, respectively. The terms $h(T_{fuel})$, $h(T_{air})$ and $h(T)$ are the ideal gas molar enthalpies for each component at the fuel, air and the exit temperatures. ΔH is the heat of reaction at reference temperature.

B. Water Gas Shift (WGS)

In the water gas shift reactor CO reacts with steam and produces hydrogen and carbon dioxide:

$$CO + H_2O \leftrightarrow CO_2 + H_2. \tag{10}$$

The reaction rate expressions for WGS is obtained from the Arrhenius equation,

$$r = K_f e^{-\frac{E_f}{RT}}[CO][H_2O] - K_b e^{-\frac{E_b}{RT}}[CO_2][H_2], \tag{11}$$

where K_f, K_b, E_f and E_b are reaction rate parameters. Again, this expression is to be used in simulations, and not for observer design.

The molar dynamics of the reactor is

$$\dot{M} = F_{gas} + F_{water} - F_{out} + q\,r\,V \tag{12}$$

where, F_{gas}, F_{water}, F_{out} are the gas, air and exit molar flow vectors respectively, and,

$$q = [0 \quad 0 \quad -1 \quad 1 \quad 1 \quad -1 \quad 0]' \tag{13}$$

from the stoichiometry of the reaction (10). Likewise, the dynamics of the temperature T is,

$$\begin{aligned}(mc_p)\dot{T} = {F_{gas}}'h(T_{gas}) + {F_{water}}'h(T_{water}) \\ -{F_{out}}'h(T) + \Delta H\,r\,V.\end{aligned} \tag{14}$$

Note that we have used the same dynamic variables (M and T) and constants (V, m, c_p and ΔH) in both CPO and WGS models. No confusion should arise, however, because the observers in the next section are derived separately for each reactor.

III. Observer Design

A. CPO Observer

We now present an observer design to estimate the unmeasured vector of molar holdups M in the model (6)-(9). Our design relies on the measurements of temperature, T, and the total pressure, P, which depends on the sum of M_i's as in the Ideal Gas Law:

$$P = \frac{RT}{V}\sum_{i=1}^{7}(M_i). \tag{15}$$

F_{fuel} and F_{air} in (6)-(9) are assumed to be known, because they depend on the compositions of air and supply fuel. F_{out}, however, depends on the unknown molar holdup vector M. Denoting by W_i, $i = 1, ..., 7$, the molecular weights, and by P_{ds} the measured downstream pressure, we express F_{out} as

$$F_{out} = \frac{c_{out}\sqrt{P - P_{ds}}}{\sum_{i=1}^{7}(M_i W_i)}M \tag{16}$$

where the numerator calculates the mass flow from the orifice equation, with orifice constant c_{out}, while division by the total mass $\sum_{i=1}^{7}(M_i W_i)$ and multiplication by the molar holdup vector M translate this mass flow to a vector of molar flows.

To design a reduced-order observer, we define the new variable

$$\xi = A\begin{bmatrix} M \\ T \end{bmatrix} \tag{17}$$

where the 6×8 matrix A is to be selected such that its rows are linearly independent, and lie in the left null space of

$$Y = \begin{bmatrix} q_1 & q_2 \\ \frac{1}{mcp}\Delta H_{POX} & \frac{1}{mcp}\Delta H_{FOX} \end{bmatrix}; \tag{18}$$

that is, $AY = 0$. Because the nonlinear reaction rates r_{pox} and r_{fox} enter the equations (6)-(9) through the matrix Y, the transformation (17) cancels them in the dynamics of ξ:

$$\begin{aligned}\dot{\xi} &= A\begin{bmatrix} F_{fuel} \\ \frac{1}{mc_p}{F_{fuel}}'h(T_{fuel}) \end{bmatrix} \\ &+A\begin{bmatrix} F_{air} \\ \frac{1}{mc_p}{F_{air}}'h(T_{air}) \end{bmatrix} - A\begin{bmatrix} F_{out} \\ \frac{1}{mc_p}{F_{out}}'h(T) \end{bmatrix}.\end{aligned} \tag{19}$$

Our task is thus to design an observer to estimate this ξ with $\hat{\xi}$, and to compute $\hat{M}$ from $\hat{\xi}$. However, because the dimensions of M and ξ do not agree, we augment ξ with the measured variables P and T, and obtain the relation

$$\begin{bmatrix} \xi \\ \frac{PV}{RT} \\ T \end{bmatrix} = \begin{bmatrix} A \\ 1\,1\,1\,1\,1\,1\,1\,0 \\ 0\,0\,0\,0\,0\,0\,0\,1 \end{bmatrix}\begin{bmatrix} M \\ T \end{bmatrix}, \tag{20}$$

where the augmented matrix is now nonsingular because the last two rows do not lie in the left null space of Y in (18) and, hence, are linearly independent from the rows of A. This means that, once $\hat{\xi}$ is obtained from a reduced-order observer, we can calculate $\hat{M}$ from

$$\begin{bmatrix} \hat{M} \\ T \end{bmatrix} = \begin{bmatrix} A \\ 1\,1\,1\,1\,1\,1\,1\,0 \\ 0\,0\,0\,0\,0\,0\,0\,1 \end{bmatrix}^{-1}\begin{bmatrix} \hat{\xi} \\ \frac{PV}{RT} \\ T \end{bmatrix}. \tag{21}$$

Our observer for system (19) is

$$\begin{aligned}\dot{\hat{\xi}} &= A\begin{bmatrix} F_{fuel} \\ \frac{1}{mc_p}{F_{fuel}}'h(T_{fuel}) \end{bmatrix} \\ &+A\begin{bmatrix} F_{air} \\ \frac{1}{mc_p}{F_{air}}'h(T_{air}) \end{bmatrix} - A\begin{bmatrix} \hat{F}_{out} \\ \frac{1}{mc_p}\hat{F}'_{out}h(T) \end{bmatrix}\end{aligned} \tag{22}$$

where, from (15), (16), $\hat{F}_{out}$ is to be calculated using

$$\hat{F}_{out} = \frac{c_{out}\sqrt{\sum_{i=1}^{7}(\hat{M}_i)\frac{RT}{V} - P_{ds}}}{\sum_{i=1}^{7}(\hat{M}_i W_i)}\hat{M}. \quad (23)$$

B. WGS Observer

Unlike the CPO model which has two reactions, the WGS contains only one. This means we can apply the same observer design procedure using only temperature measurements.
For this observer we define

$$\zeta = \tilde{A}\begin{bmatrix} M \\ T \end{bmatrix} \quad (24)$$

where the 7×8 matrix $\tilde{A}$ is to be selected such that its rows are linearly independent, and lie in the left null space of

$$\tilde{Y} = \begin{bmatrix} q \\ \frac{1}{mcp}\Delta H \end{bmatrix}. \quad (25)$$

Because $\tilde{A}\tilde{Y} = 0$, the transformation (24) cancels the reaction rate r in the ζ model:

$$\dot{\zeta} = \tilde{A}\begin{bmatrix} F_{gas} \\ \frac{1}{mc_p}{F_{gas}}'h(T_{gas}) \end{bmatrix} \quad (26)$$

$$+\tilde{A}\begin{bmatrix} F_{water} \\ \frac{1}{mc_p}{F_{water}}'h(T_{water}) \end{bmatrix} - \tilde{A}\begin{bmatrix} F_{out} \\ \frac{1}{mc_p}{F_{out}}'h(T) \end{bmatrix}.$$

Similar to the derivations in the previous section, we obtain $\hat{M}$ from $\hat{\zeta}$, using

$$\begin{bmatrix} \hat{M} \\ T \end{bmatrix} = \begin{bmatrix} \tilde{A} \\ 0\,0\,0\,0\,0\,0\,0\,1 \end{bmatrix}^{-1}\begin{bmatrix} \hat{\zeta} \\ T \end{bmatrix}. \quad (27)$$

Likewise, the observer for ζ is

$$\dot{\hat{\zeta}} = \tilde{A}\begin{bmatrix} F_{gas} \\ \frac{1}{mc_p}{F_{gas}}'h(T_{gas}) \end{bmatrix} \quad (28)$$

$$+\tilde{A}\begin{bmatrix} F_{water} \\ \frac{1}{mc_p}{F_{water}}'h(T_{water}) \end{bmatrix} - \tilde{A}\begin{bmatrix} \hat{F}_{out} \\ \frac{1}{mc_p}\hat{F}'_{out}h(T) \end{bmatrix}.$$

where $\hat{F}_{out}$ is computed as in (23).

C. Convergence Analysis

We now show that the observer designs of Sections III-A and III-B ensure convergence around operating points of physical interest. Although our analysis in this section is local, simulation studies in the next section indicate large regions of attraction. To analyze convergence properties of the WGS observer (27)-(28), we let the 7×7 matrix $\tilde{A}_1$, and the 7×1 vector $\tilde{A}_2$, denote partitions of

$$\tilde{A} = [\tilde{A}_1 \quad \tilde{A}_2], \quad (29)$$

and obtain from (27),

$$\hat{M} = {\tilde{A}_1}^{-1}\hat{\zeta} - {\tilde{A}_1}^{-1}\tilde{A}_2 T. \quad (30)$$

Thus, from (26) and (28), the observer error

$$e := \hat{M} - M = {\tilde{A}_1}^{-1}(\hat{\zeta} - \zeta) \quad (31)$$

is governed by

$$\begin{aligned} \dot{e} &= {\tilde{A}_1}^{-1}\tilde{A}\begin{bmatrix} \hat{F}_{out} - F_{out} \\ \frac{1}{mc_p}h(T)'(\hat{F}_{out} - F_{out}) \end{bmatrix} \quad (32) \\ &= -(I + {\tilde{A}_1}^{-1}\tilde{A}_2\frac{1}{mc_p}h(T)')(\hat{F}_{out} - F_{out}), \end{aligned}$$

where F_{out} depends on M as in (23). This means that the local stability of the equilibrium $e = 0$ is determined by the Jacobian matrix

$$J_{WGS} = -(I + {\tilde{A}_1}^{-1}\tilde{A}_2\frac{1}{mc_p}h(T)')\frac{\partial F_{out}}{\partial M}, \quad (33)$$

which is indeed Hurwitz (see Tables III and IV in Section 4) when evaluated at physically relevant operating points of (M, T). Similar calculations for the CPO observer shows that its convergence properties depend on the Jacobian matrix

$$\begin{aligned} J_{CPO} &= \quad (34) \\ &- \Sigma\bar{A}_1 \begin{bmatrix} (I + {\bar{A}_1}^{-1}\bar{A}_2\frac{1}{mc_p}h(T)')\frac{\partial F_{out}}{\partial M} \end{bmatrix}{\bar{A}_1}^{-1}\Sigma' \end{aligned}$$

where $\bar{A}_1$ and $\bar{A}_2$ are, respectively, 7×7 and 7×1 matrices obtained from the partition

$$\begin{bmatrix} A \\ 1\ 1\ 1\ 1\ 1\ 1\ 1\ 0 \end{bmatrix} = \begin{bmatrix} \bar{A}_1 & \bar{A}_2 \end{bmatrix}, \quad (35)$$

and $\Sigma = \begin{bmatrix} I_{6\times 6} & 0_{6\times 1} \end{bmatrix}$.

The difference of the expressions (33) and (34) is because the CPO observer in (34) uses two measurements and, hence, its order is 6, whereas the WGS observer uses one measurement and has order 7. The stability of J_{CPO} is also established in Section 4, Tables I and II, for several operating points.

IV. Simulation Results

A. CPO Observer

We first present simulation results for the CPO observer derived in Section III-A. For these simulations we implement the model equations (6)-(9) in MATLAB SIMULINK with reference values $F_{fuel} = 0.7229$ (mole/sec), $T_{fuel} = 623.15$ (K), $F_{air} = 1.9850$ (mole/sec), $T_{air} = 557.25$ (K), obtained from data for a stationary fuel cell power plant. The observer takes CPO total pressure and temperature as measured outputs. Figures 1 from (a) to (g) show convergence of the mole fraction estimates for each species(dashed) to their true values (solid), and Figure 1 (h) shows convergence of the outflow, $\hat{F}_{out}$ to F_{out}. At $t = 100s$, inlet fuel flow is increased by 20 percent, and at $t = 200s$ air supply is increased by 20 percent. Despite the resulting transients, the observer estimates again converge to the true values. Indeed, Tables I and II show the stability of the Jacobian matrices at the steady-state values resulting from several reference values of F_{fuel} and F_{air}, including those employed in our simulations.

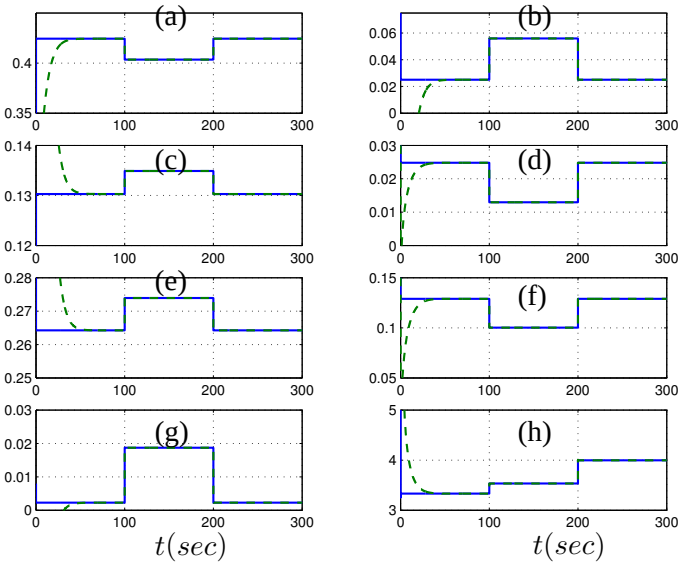

Fig. 1. CPO Observer simulation results: Mole fraction of a)N2, b)CH4, c)CO , d)CO2, e)H2, f)H2O, g)O2, h) Out Flow (mole/sec).

B. WGS Observer

We next present simulation results for the WGS observer, derived in Section III-B . The observer takes WGS temperature as the measured output. Figures 2 (a) to (g) show convergence of the mole fraction estimates for each species (dashed), to their true values (solid), and Figure 2 (h) shows convergence of the outflow. At $t = 100s$ inlet gas flow is increased by 20 percent, and at $t = 200s$ water supply is increased by 20 percent. Tables III and IV shows the stability of the Jacobian matrices at the steady-state values resulting from several reference values of F_{gas} and F_{water}. We note from these tables that the Jacobian has no slow poles, which is consistent with the fast convergence of the observer in simulations.

V. Conclusions

In this study, we have designed reduced-order observers for fuel cell FPS reactors, CPO and WGS. The observers estimate chemical composition (mole fraction of each species in the stream) without knowledge of reaction rate expressions. Because these designs rely on stoichiometric coefficients to cancel the reaction rates, they require as many measured outputs as the number of reactions. Indeed we have employed two outputs (temperature and pressure) for the CPO, which contains the POX and FOX reactions; and only one output (temperature) for the WGS, which contains the shift reaction. The performance of the observers are studied with simulation results.

For future study we plan to investigate the robustness of these designs to the uncertainty in stoichiometric coefficients, and to the side reactions in the CPO which are not modelled in this paper. Because we calculate flows from orifice equations, rather than measure them, an important task is to validate and fine-tune these equations with experimental data.

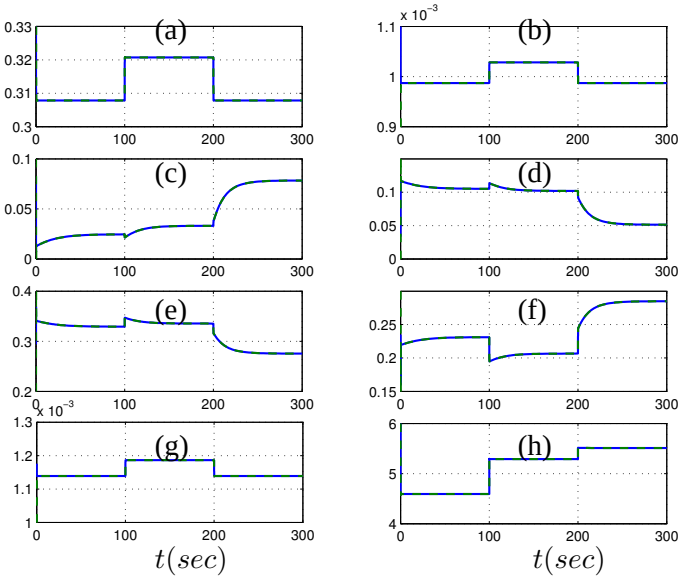

Fig. 2. WGS Observer simulation results: Mole fraction of a)N2, b)CH4, c)CO , d)CO2, e)H2, f)H2O, g)O2, h) Out Flow (mole/sec).

F_{fuel}	.578	.7229	.867
$\lambda_{J_{CPO}}$	$-2.43 \cdot 10^{-1}$	$-1.5 \cdot 10^{-1}$	$-7.6 \cdot 10^{-2}$
	$-4.73 \cdot 10^{2}$	$-2.8 \cdot 10^{2}$	$-1.4 \cdot 10^{2}$
	$-2.35 \cdot 10^{2}$	$-1.4 \cdot 10^{2}$	$-6.9 \cdot 10^{1}$
	$-2.35 \cdot 10^{2}$	$-1.4 \cdot 10^{2}$	$-6.9 \cdot 10^{1}$
	$-2.35 \cdot 10^{2}$	$-1.4 \cdot 10^{2}$	$-6.9 \cdot 10^{1}$
	$-2.35 \cdot 10^{2}$	$-1.4 \cdot 10^{2}$	$-6.9 \cdot 10^{1}$
	$-2.35 \cdot 10^{2}$	$-1.4 \cdot 10^{2}$	$-6.9 \cdot 10^{1}$

TABLE I

Eigenvalues of J_{CPO} in (34) for $F_{air} = 1.985$ (mole/sec) and varying values of F_{fuel}.

F_{air}	1.588	1.985	2.382
$\lambda_{J_{CPO}}$	$-4.8 \cdot 10^{-2}$	$-1.5 \cdot 10^{-1}$	$-2.7 \cdot 10^{-1}$
	$-8.72 \cdot 10^{1}$	$-2.8 \cdot 10^{2}$	$-5.22 \cdot 10^{2}$
	$-4.36 \cdot 10^{1}$	$-1.4 \cdot 10^{2}$	$-2.6 \cdot 10^{2}$
	$-4.36 \cdot 10^{1}$	$-1.4 \cdot 10^{2}$	$-2.6 \cdot 10^{2}$
	$-4.36 \cdot 10^{1}$	$-1.4 \cdot 10^{2}$	$-2.6 \cdot 10^{2}$
	$-4.36 \cdot 10^{1}$	$-1.4 \cdot 10^{2}$	$-2.6 \cdot 10^{2}$
	$-4.36 \cdot 10^{1}$	$-1.4 \cdot 10^{2}$	$-2.6 \cdot 10^{2}$

TABLE II

Eigenvalues of J_{CPO} in (34) for $F_{fuel} = .7229$ (mole/sec) and varying values of F_{air}.

F_{gas}	2.7891	3.4864	4.1837
$\lambda_{J_{WGS}}$	$-1.42 \cdot 10^{6}$	$-1.32 \cdot 10^{6}$	$-1.21 \cdot 10^{6}$
	$-2.9 \cdot 10^{1}$	$-3.74 \cdot 10^{1}$	$-4.57 \cdot 10^{1}$
	$-1.61 \cdot 10^{1}$	$-2.1 \cdot 10^{1}$	$-2.58 \cdot 10^{1}$
	$-1.61 \cdot 10^{1}$	$-2.1 \cdot 10^{1}$	$-2.58 \cdot 10^{1}$
	$-1.61 \cdot 10^{1}$	$-2.1 \cdot 10^{1}$	$-2.58 \cdot 10^{1}$
	$-1.61 \cdot 10^{1}$	$-2.1 \cdot 10^{1}$	$-2.58 \cdot 10^{1}$
	$-1.61 \cdot 10^{1}$	$-2.1 \cdot 10^{1}$	$-2.58 \cdot 10^{1}$

TABLE III

Eigenvalues of J_{WGS} in (33) for $F_{water} = 1.1056$ (mole/sec) and varying values of F_{gas}.

F_{water}	.8844	1.1056	1.3267
$\lambda_{J_{WGS}}$	$-8.9 \cdot 10^{5}$	$-1.32 \cdot 10^{6}$	$-1.54 \cdot 10^{6}$
	$-2.37 \cdot 10^{1}$	$-3.74 \cdot 10^{1}$	$-4.69 \cdot 10^{1}$
	$-1.29 \cdot 10^{1}$	$-2.1 \cdot 10^{1}$	$-2.69 \cdot 10^{1}$
	$-1.29 \cdot 10^{1}$	$-2.1 \cdot 10^{1}$	$-2.69 \cdot 10^{1}$
	$-1.29 \cdot 10^{1}$	$-2.1 \cdot 10^{1}$	$-2.69 \cdot 10^{1}$
	$-1.29 \cdot 10^{1}$	$-2.1 \cdot 10^{1}$	$-2.69 \cdot 10^{1}$
	$-1.29 \cdot 10^{1}$	$-2.1 \cdot 10^{1}$	$-2.69 \cdot 10^{1}$

TABLE IV

Eigenvalues of J_{WGS} in (33) for $F_{gas} = 3.4864$ (mole/sec) and varying values of F_{water}.

REFERENCES

[1] M. Arcak, H. Gorgun, L.M. Pedersen, and S. Varigonda, *A nonlinear observer design for fuel cell hydrogen estimation*, IEEE Transactions on Control Systems Technology **12** (2004), 101–110.

[2] G. Bastin and D. Dochain, *On-line estimation and adaptive control of bioreactors*, Elseveir, Amsterdam-Oxford-New York-Tokyo, 1990.

[3] L.J.M.J Blomen and M.N. Mugerwa, *Fuel cells systems*, Plenum Press, New York, 1993.

[4] L. Carette, K.A. Friedrich, and U. Stimming, *Fuel cells - fundamentals and applications*, Fuel Cells Journal **1** (2001), 5–39.

[5] J.P. Gauthier, H. Hammouri, and S. Othman, *A simple observer for nonlinear systems applications to bioreactors*, IEEE Transactions on Automatic Control **37** (1992), 875–880.

[6] A.M. Gibon-Fargeot, H. Hammouri, and F. Celle, *Nonlinear observers for chemical reactors*, Chemical Engineering Science **49** (1994), 2287–2300.

[7] R.S. Glass, *Sensor needs and requirements for proton-exchange membrane fuel cell systems and direct-injection engines*, Lawrence Livermore National Laboratory, Applied Energy Technologies Program, 2000.

[8] Parsen Inc., *Fuel cells: A handbook*, Elsevier, Business/Technology Books, 2000.

[9] N.M. Iyer and A.E. Farell, *Design of a stable adaptive nonlinear observer for an exothermic stirred tank reactor*, Computers and Chemical Engineering **20** (1996), no. 9, 1141–1147.

[10] A.J. Krener and A. Isidori, *Linearization by output injection and nonlinear observers*, Systems and Control Letters **3** (1998), 47–52.

[11] J. Larminie and A. Dicks, *Fuel cell systems explained*, John Wiley and Sons, Inc., 2000.

[12] L. Limqueco, J.C. Kantor, and S. Harvey, *Nonlinear adaptive observation of an exothermic stirred-tank reactor*, Chemical Engineering Science **46** (1991), 797–805.

[13] L.C. Limqueco and J.C. Kantor, *Nonlinear output feedback control of an exothermic reactor*, Computers and Chemical Engineering **14** (1990), 427–437.

[14] J.T. Pukrushpan, A.G. Stefanopoulou, S. Varigonda, L.M. Pedersen, S. Ghosh, and H. Peng, *Control of natural gas catalytic partial oxidation for hydrogen generation in fuel cell applications*, Proceedings of the American Control Conference (Denver, Colorado), 2003, pp. 2030–2036.

[15] C. Song, *Fuel processing for low-temperature and high-temperature fuel cells challenges, and opportunities for sustainable development in the 21st century*, Catalysis Today **77** (2002), 17–49.

[16] M. Soroush, *Nonlinear state-observer design with application to reactors*, Chemical Engineering Science **52** (1997), no. 3, 387–404.

[17] ———, *State and parameter estimations and their applications in process control*, Computers and Chemical Engineering **23** (1998), 229–245.